J Therm Anal Calorim (2010) 101:729–735
DOI 10.1007/s10973-010-0814-9

Formation and some properties of barium titanate embedded into porous matrices

V. V. Sidorchuk · V. A. Tertykh · V. P. Klimenko · A. V. Ragulya

IVMTT2009 Special Chapter

Abstract Embedding of barium titanate into porous oxide matrices via sol–gel synthesis and introduction in structured slurry based on fumed oxides has been carried out. Prepared compositions have been studied using XRD, DTA-TG, FTIR, TEM, and adsorption of nitrogen. It has been established that simultaneous formation both barium titanate crystal structure and porous structure of matrices occurs. Crystallites of barium titanate, which arise in pores, possess lesser size in comparison with that for bulk $BaTiO_3$.

Keywords Barium titanate · Barium titanyl oxalate · Porous matrices · Sol–gel process · Confinement effect

Introduction

The perovskite family includes many titanates, in part barium titanate, used in various electroceramic applications, for example, electronic, electrooptical, and electromechanical applications of ceramics (mutilayer capacitors, positive temperature coefficient thermistors, piezoelectric transducers, and variety electrooptic devices) [1, 2]. These compounds is also interesting as catalysts of the complete oxidation, photocatalysts, and catalyst carriers, sensitive elements for gas and water vapor sensors [3–6].

It is well known that embedded or formed in porous matrices particles of various substances possess singular physical, chemical, catalytic properties owing to achievement of nanodispersed state and limiting influence of pore walls on enlargement of particles (confinement effect) [7]. This approach is also perspective for barium titanate, a typical ferroelectric and photocatalyst. There are a few works which are devoted to synthesis of barium titanate in pores and study its properties, but contradictory results were obtained [8–11]. Thus, Kinka et al. [9] confirmed incorporation of barium titanate into mesoporous silica MCM-41 (pore diameter 2.0-3.7 nm), but no phase transition from paraelectric to ferroelectric was observed due to the particle size being smaller than the critical size. On the other hand, a decrease in dielectric constant maximum temperature from 130 to 55 °C (dielectric quantum-confinement effect) was observed for barium titanate mesocrystals smaller than 3 nm in uniform mesopores of the MCM-41 silica [8].

Study of embedding of barium titanate into porous oxide matrices of different nature and investigation of some physicochemical properties of the synthesized compositions was the aim of this work.

Experimental procedure

Barium titanyl oxalate (BTO) as a precursor and barium titanate (BT) with the specific surface area $S = 23$ m^2 g^{-1} (both ferro), tetraethoxysilane TEOS (Fluka), pyrogenic silicas with the specific surface area 380 and 50 m^2 g^{-1}

V. V. Sidorchuk
Institute for Sorption and Endoecology Problems of National Academy of Sciences of Ukraine, 13, General Naumov Str., 03164 Kyiv, Ukraine

V. A. Tertykh (✉)
O.O. Chuiko Institute of Surface Chemistry of National Academy of Sciences of Ukraine, 17, General Naumov Str., 03164 Kyiv, Ukraine
e-mail: tertykh@voliacable.com

V. P. Klimenko · A. V. Ragulya
I.N. Frantsevich Institute for Problems of Materials Science of National Academy of Sciences of Ukraine, 3, Krzhyzhanovsky Str., 03142 Kyiv, Ukraine

(A-380 and A-50), titania and alumina with the specific surface area 64 and 89 $m^2\ g^{-1}$, respectively (Oriana, Ukraine), were used as raw materials. Silica and alumina were X-ray amorphous, titania is composed of aggregates of crystallites of anatase and rutile.

We have prepared barium titanate particles embedded in porous inorganic matrices in two stages. The first stage consists in incorporation of the precursor—BTO—into pores of some oxides. This procedure was realized using ultrasonic treatment (20 kHz, 80 °C) via:

(i) application of the condensation method—by means of sol–gel technique namely by the way hydrolysis-condensation of tetraethoxysilane in the aqueous-alcohol medium in the BTO presence. Routine method was following: 20 mL of TEOS, 8 mL of ethanol, and 1 mL of acetic acid (catalyst of hydrolysis) were stirred via sonification for 10 min, 16 mL of water was added and agitation lasted 10 min, 2.4 g of BTO (or corresponding amount of barium titanate) were added and this mixture was stirred 10 min. Obtained sol was turned into gel either at 25 °C on air during 24 h or through solvothermal treatment in an autoclave for 3 h;

(ii) preparation of aqueous structured slurry (dispersion) with nonporous fumed silica, alumina, or titania; typical procedure was following: 2.9 g of TiO_2 were dispersed in 10 mL of water during 10 min, 2.0 g of BTO were introduced into obtained dispersion, extra 1.5 g of TiO_2 were added and agitation continues 10 min.

All prepared gels and structured slurries were dried on air at 20 °C for 40 h. Both synthetic strategies ensure simultaneous porous structure formation and embedding of BTO (or barium titanate) into pores.

The second stage includes BTO thermodestruction and barium titanate origination in pores of the different matrices with pore size of 1–73 nm. Such pores serve as nanoreactors. As a result, size of emerging barium titanate crystals is determined by pore diameter and particle growth is suppressed at the elevated temperature.

Properties of compositions prepared using both above-mentioned stages were studied by XRD, DTA-TG, FTIR, TEM, and nitrogen adsorption techniques. The phase composition (XRD) of the obtained samples was determined with diffractometer PW 1830 (Philips) using Cu Kα radiation. Thermogravimetric analysis was made using Derivatograph-Q (MOM, Budapest) in the temperature range 20–800 °C with the heating rate—10°/min. Weight of samples was 150 mg. The specific surface area was calculated using the BET method from adsorption–desorption isotherms of nitrogen (NOVA-1200, Quantochrome Instruments). The FTIR spectra in the range 4000–500 cm^{-1} were registered using spectrophotometer Spectrum-One (Perkin-Elmer). The ratio of sample and KBr in the pellets was 1:20.

Results and discussion

Decomposition of BTO in pores of all used matrices occurs equally and in full accordance with the scheme proposed for thermodestruction of bulk BTO [12–14]:

$$BaTiO(C_2O_4)_2 \cdot 4H_2O \overset{370\,^\circ C}{\rightarrow} BaTiO(C_2O_4)_2 \overset{550\,^\circ C}{\rightarrow} BaCO_3 + TiO_2 \overset{710\,^\circ C}{\rightarrow} BaTiO_3$$

This can see from course of DTA and TG curves for three samples (Fig. 1a–c). However, temperature of endoeffect corresponding to the third stage is slightly lower than that for bulk BTO and effect, which confirms the second stage, was very weak. Besides, additional endoeffect on DTA curve about 150 °C presents. It appears owing to overlapping of processes water loss of BTO and removal of adsorbed water from porous space of the matrix.

XRD data of composites indicate formation of pure BT phase in the structure of all matrices after thermal treatment at 800 °C (Fig. 2). From these data, it follows that for the sample prepared on the basis of amorphous silica matrix all BT reflexes are present on the halo background, but for crystalline matrices X-ray patterns are defined as a superposition of barium titanate, crystalline TiO_2 and Al_2O_3.

FTIR spectra of compositions also indicate BT formation. Thus, weak absorption bands of bulk BT at 475, 860, 930 and 975 cm^{-1} were detected in spectra, although these bands are partially overlapped with bands of oxide matrices.

TEM micrographs confirm XRD results. For the composite prepared by sol–gel method from TEOS and BTO at 150 °C and treated at 680 °C (Fig. 3a and b), crystals of barium titanate and their aggregates with size of 10–50 nm can be seen in the amorphous silica matrix.

On the other hand, size of BT crystals calculated using the Debye–Sherrer equation in the direction of 101 plane D_{101} (this reflex is the most intensive) is equal to 14 nm. At the same time particles of the regular spherical form with size of 20–50 nm are observed in micrograph of the sample based on fumed titania prepared by dispersion in water with addition of the appropriate amount of BTO, drying and calcination at 680 °C (Fig. 3c and d). Inside of these particles, there are fine barium titanate crystals (the size of 5–10 nm) covered titania shell. Slightly expressed reflexes of BT (crystallite size $D_{101} = 9$ nm) are seen at diffractogram of this sample. After thermal treatment at 800 °C intensities of all these reflexes are essentially enhanced and the diffractogram represents a superposition of titanium dioxide (anatase, rutile) and barium titanate reflexes as was

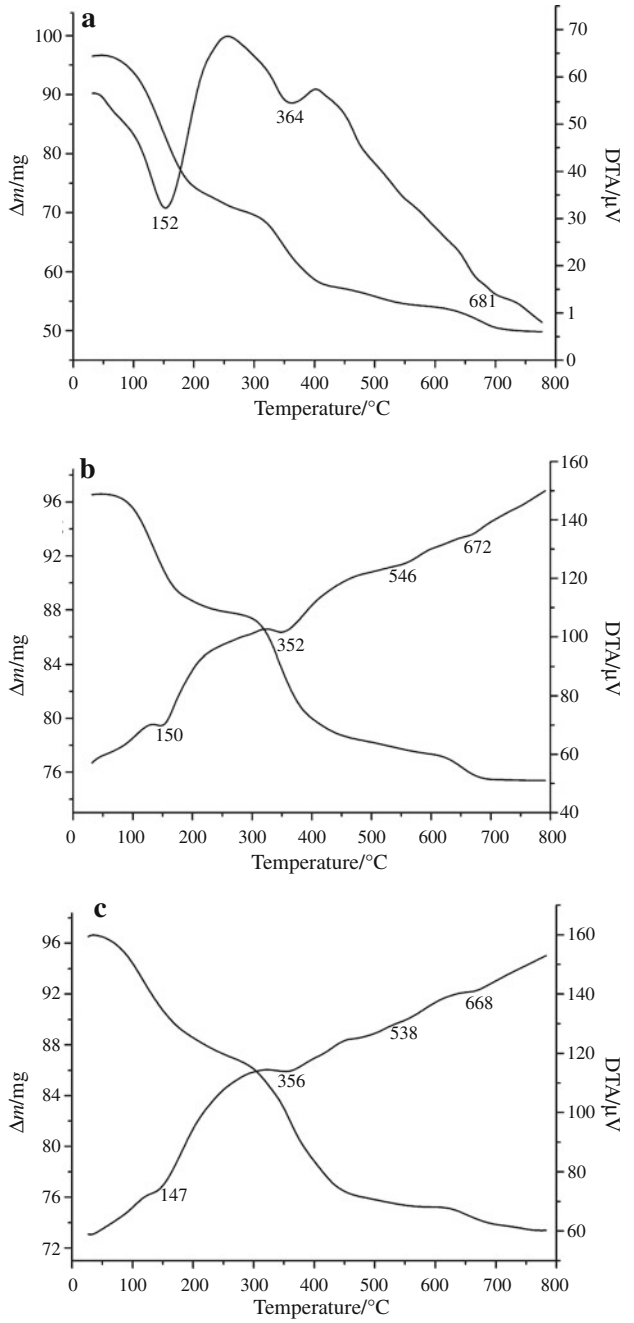

Fig. 1 DTA–TG curves of BTO/SiO_2 composite—sample N2 (hereinafter, numbers of samples from the Table 1) prepared via sol–gel method (**a**), BTO/SiO_2 composite - sample N15 prepared on basis of fumed silica A-380 (**b**), BTO/TiO_2 composite—sample N18 prepared on basis of fumed titania (**c**)

indicated (Fig. 2c). D_{101} magnitude of barium titanate for the last sample is equal to 12 nm. Thus, elevation of the calcination temperature is favorable for the definite (though petty) increase of the crystallite size due to collecting recrystallization processes.

The peak corresponding to 101 plane of barium titanate is also the most intensive in the sample based on alumina

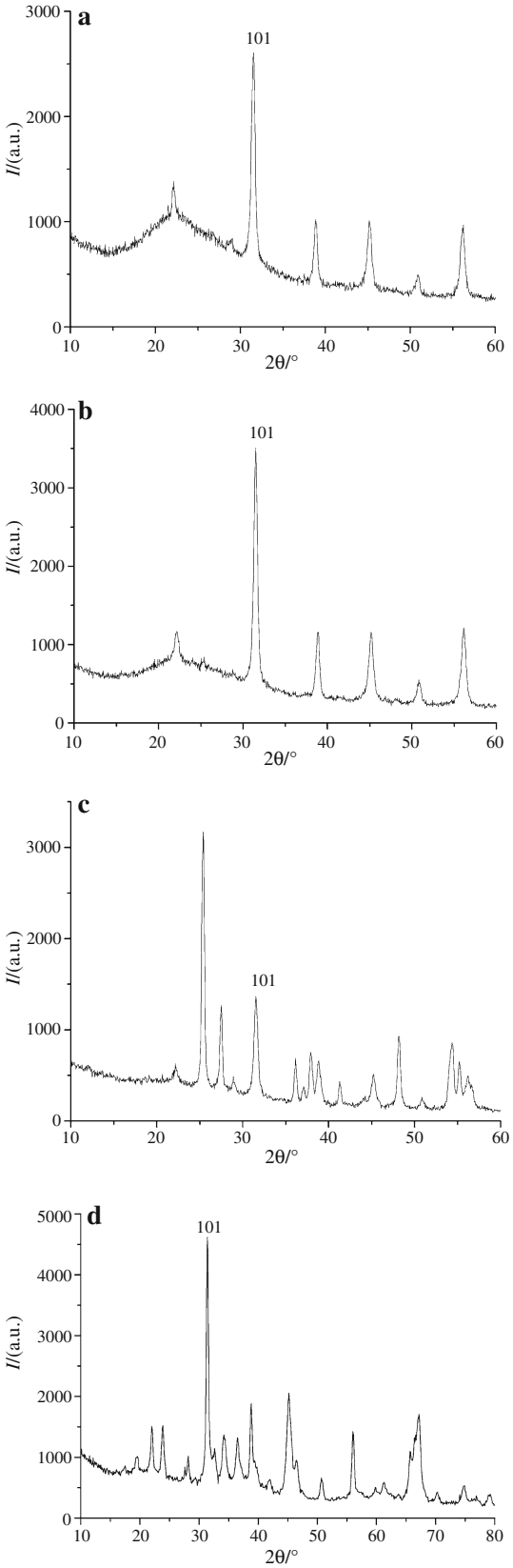

Fig. 2 Diffractograms of BT/SiO_2 composites—samples N3 (**a**), N16 (**b**); BT/TiO_2 composite —sample N19 (**c**); BT/Al_2O_3 composite—sample N23 (**d**)

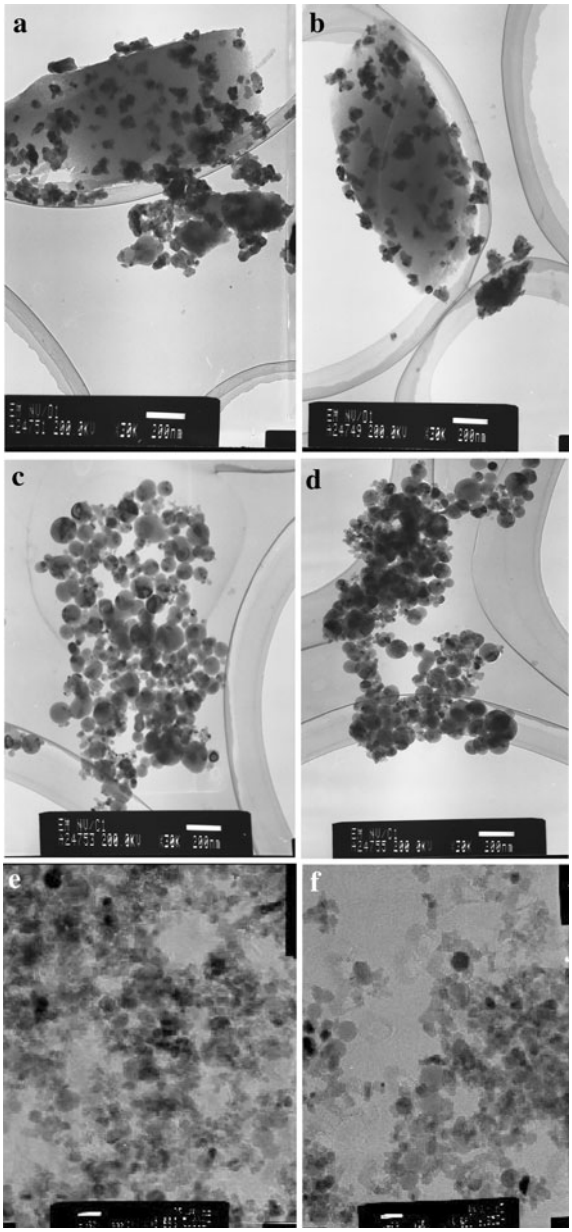

Fig. 3 TEM micrographs of BTO/SiO_2 (**a**, **b**), BTO/TiO_2 (**c**, **d**), and BT/Al_2O_3 (**e**, **f**) composites

and the least intensive—for the BT/titania composite. Besides, this magnitude was also maximum for the BT/alumina composite after annealing at 800 °C (D_{101} = 24 nm). It is clear from these experimental data that more perfect BT structure is formed in the Al_2O_3 matrix. TEM micrographs of this composite (Fig. 3e and f) are similar to the sample based on fumed titania (Fig. 3c and d).

Account must be taken that the crystallite size D_{101} for the bulk barium titanate obtained by thermal destruction of BTO at 700 °C is equal to 17 nm. It is obviously that we can talk about increasing of dispersity of barium titanate which is formed from BTO in pores of the silica and titania

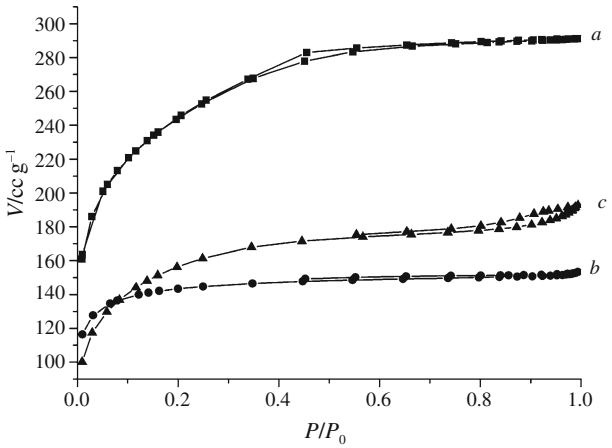

Fig. 4 Adsorption–desorption isotherms of nitrogen for pure SiO_2 prepared via sol–gel method (*a*), BTO/SiO_2 composite prepared via sol-gel method—sample N2 (*b*), and BT/SiO_2 composite—sample N3 (*c*)

matrices. Conversely, more large-sized BT crystallites are formed in the alumina matrix in comparison with particles of bulk BT prepared at BTO thermal destruction in the same conditions. FTIR spectra of the obtained composites confirm BT formation in pores of matrices via thermodestruction of BTO.

Proposed approach for the composites synthesis simultaneously with BT crystallization provides formation of the matrix porous structure (Fig. 4). The availability of BT or its precursor (BTO) in the gels or in the structured dispersions was shown to effect essentially on parameters of the porous structure which is formed on the stage of the gel desiccation in comparison with porous structure of the pure matrices (Table 1). Following precursor thermodestruction in the matrix also essentially changes porous structure of the composite.

Some peculiarities of such transformations of the porous structure parameters were detected depending on method of the composite synthesis, namely:

(1) Introducing BTO or BT at the sol–gel synthesis leads to an increase of sorption (V_s) and total (V_Σ) pore volume. Opposite, thermal treatment of silica/BTO composites results in a decrease of V_s and V_Σ magnitudes. The latter can be associated with onset of solid phase (silica network) owing to hydrolysis processes of TEOS and polycondensation of the intermediate. It is quite possible that availability BTO (or BT) crystallites in the reaction mixture leads to a decrease of packing compactness of the primary sol globules.

(2) At the dispersion (mulling) synthesis exactly the opposite tendencies take place: xerogels of the matrix/BTO(BT) composites have the less magnitudes of pore volume compared with pure matrices. It is obviously that in this case gel network is formed via

Table 1 Parameters of porous structure of carriers and their composites with barium titanyl oxalate (BTO) and barium titanate (BT)

No.	Samples and preparation conditions	Specific surface area, $S/m^2\ g^{-1}$	Total pore volume, $V_\Sigma/cm^3\ g^{-1}$	Pore diameter, d/nm
1	Silica from TEOS, 20 °C	640	0.12	0.8
2	Silica from TEOS with 38.5% BTO, 20 °C	231	0.24	4.2
3	N2 + thermal treatment at 800 °C	221	0.22	4.0
4	Silica from TEOS with 77% BTO, 20 °C	5	0.40	320
5	N4 + thermal treatment at 800 °C	19	0.15	31.6
6	Silica from TEOS with 20% BT, 20 °C	31	0.31	40.0
7	Silica from TEOS with 40% BT, 20 °C	16	0.13	32.5
8	Silica from TEOS, 150 °C	620	0.23	1.5
9	Silica from TEOS with 38.5% BTO, 150 °C	191	0.42	8.8
10	N9 + thermal treatment at 800 °C	22	0.32	58.2
11	Aerosilogel from fumed silica A-50	48	0.61	50.8
12	Aerosilogel from fumed silica A-50 with 38.5% BTO	30	0.40	53.3
13	N12 + thermal treatment at 800 °C	42	0.55	52.4
14	Aerosilogel from fumed silica A-380	355	0.98	11.0
15	Aerosilogel from fumed silica A-380 with 38.5% BTO	215	0.65	12.1
16	N15 + thermal treatment at 800 °C	290	0.89	12.3
17	Titania gel from fumed TiO_2	61	0.54	35.4
18	Titania gel with 38.5% BTO	48	0.33	27.5
19	N18 + thermal treatment at 800 °C	23	0.42	73.0
20	Titania gel with 20% BT	42	0.47	44.8
21	Alumina gel from fumed Al_2O_3	81	0.41	20.2
22	Alumina gel with 38.5% BTO	70	0.58	33.1
23	N22 + thermal treatment at 800 °C	42	0.73	69.5

d, Average pore size calculated by the formula: $d = (4\ V_\Sigma/S) \times 10^3$/nm

joining of the ready silica globules and, hence, BTO (or BT) phase fills the originated pore volume. At the same time, because of thermal destruction of BTO in pores their volume essentially increases and this enhancement varies directly with an increase of density of the substance incorporated into pores (or more precisely, with difference in BT and BTO densities). In this case, it is possible appearance of macropores in the composite structure. As a result, the total pore volume V_Σ (including micro- and mesopores as well as macropores), determined by impregnation of granules with liquid water, will be greater than sorption pore volume V_s (including only micro- and mesopores), calculated from isotherms of nitrogen adsorption from the gaseous phase. Typical adsorption isotherms, measured for the samples based on fumed silica A-380 (samples 14–16 in the Table 1), illustrate the foregoing peculiarities of porous structure formation of composites at the dispersion synthesis (Fig. 5). Shift of the location of the capillary condensation hysteresis to the range of the more high relative pressures of adsorbate for the sample with barium titanate incorporated into its structure testifies about more high pores size in comparison with pure silica.

Because the samples obtained by sol–gel method are more fine-porous, at their thermal treatment up to 800 °C in parallel with the BTO destruction the sintering processes take place. It results in a decrease of porosity of the obtained silica/barium titanate composites. It seems likely that these experimental data are important for the preparation of dense ceramics on the basis of such composites.

Thus, the synthesized samples with incorporated barium titanate remain porous ones as the starting oxide matrices. Even the more wide-porous composites based on fumed oxides at calcination up to 1250 °C (temperature is close to temperature of ceramics preparation) were sintered practically completely and lost their porosity. For example, temperature dependence of total pores volume for pure aerosilogel and composite based on fumed silica A-380 and BTO is presented in the Table 2.

It can be seen that up to 800 °C pores volume of the composite is increased as a result of the BTO thermal destruction, at more high temperatures V_Σ magnitudes are

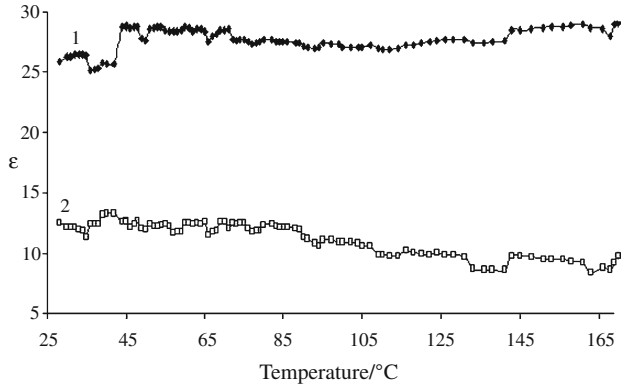

Fig. 5 Dependence of permittivity ε_1 (*1*) and dielectric losses ε_2 (*2*) for sample N16 on temperature

Table 2 Effect of the temperature treatment on the total pore volume of silica and silica/barium titanate composite

SiO_2	V_Σ/cm^3 g^{-1}	0.98	0.90	0.84	0.29	0.00
	T/°C	20	700	800	1100	1250
SiO_2/BTO	V_Σ/cm^3 g^{-1}	0.65	0.82	0.89	0.20	0.03
	T/°C	20	700	800	1100	1250

monotonically decreased and after treatment at 1250 °C both pure silica and composite with incorporated barium titanate are transformed into practically nonporous materials.

Sample of the composite obtained from fumed silica at 800 °C even in form of powder pressed up to density of 2.5 g cm^{-3}, has dielectric constant magnitudes $\varepsilon_1 = 25$–30 at the measurement in the ultrahigh frequency range (10 GHz). Besides, there is paraelectric–ferroelectric phase transition (the Curie point) on the curves of temperature dependences of dielectric constant ε_1 and dielectric losses ε_2 near 130 °C (Fig. 5). This experimental result testifies about possibility of application of such type composites as electroceramic materials.

It is well known that barium titanate is a typical photocatalyst [4, 5]. We have estimated activity of matrix/barium titanate composites in a model reaction of photodestruction of such organic dye as Safranin T in the aqueous solutions. Obtained composites was shown to possess greater photocatalytic activity in the process of Safranin T degradation in comparison with bulk BT. Bulk BT synthesized through usual thermodestruction of BTO has sufficiently lower activity—the rate constant of photodegradation $K_d = 2.3 \times 10^{-4}$ s^{-1}. For composites with BT embedded into matrix K_d exceeds in 2–3 times this value for bulk BT. Besides samples of composites possessing high-specific surface area and porosity additionally remove dye from solutions owing to adsorption processes.

Obtained matrix/BTO samples (pores volume $V_\Sigma = 0.24$–0.65 cm^3 g^{-1}) after annealing at 700 °C are transformed into less (sol–gel method, $V_\Sigma = 0.15$–0.32 cm^3 g^{-1}, pore size $d = 4$–32 nm) or more porous samples (structured slurry method, $V_\Sigma = 0.42$–0.89 cm^3 g^{-1}, $d = 12$–73 nm) of matrix/barium titanate composites. Crystallite sizes of the formed barium titanate for all samples are equal to 8–12 nm and they are slightly increased at temperature elevation up to 1100 °C.

TEM data demonstrate formation aggregates of barium titanate crystallites (10–50 nm) in the silica amorphous matrix (sol–gel method). Spherical particles (20–50 nm) consisted of 5–10 nm barium titanate crystallites coated with titania shell are formed during dispersion of BTO and TiO_2 in water and following annealing at 680 °C.

Conclusions

1. Possibilities of barium titanate preparation in pores of oxide matrices were demonstrated using different precursors and diverse approaches to synthesis of such composites.
2. Transformations of porous and crystalline structure of the composites on the miscellaneous stages of synthesis were studied by different physicochemical methods.
3. Possibilities of application of obtained composites as electroceramic materials and photocatalysts were roughly estimated.

References

1. Rae A, Chu M, Ganine V. Barium titanate: past, present and future. Ceram Trans. 2007;100:1–12.
2. Luxová J, Šulcová P, Trojan M. Study of perovskite compounds. J Therm Anal Calorim. 2008;93:823–7.
3. Moreno J, Dominguez JM, Montoya A. Synthesis and characterization of $MTiO_3$ (M = Mg, Ca, Sr, Ba) sol–gel. J Mater Chem. 1995;5:509–12.
4. Li QS, Domen K, Naito S. Photocatalytic synthesis and photodecomposition of ammonia over $SrTiO_3$ and $BaTiO_3$ based catalysts. Chem Lett. 1983;3:321–4.
5. Yohichi Y, Masaru T, Masato K. Synthesis RuO_2-loaded $BaTinO_{2n+1}$ ($n = 1, 2, 5$) using a polymerizable complex method and its photocatalytic activity for the decomposition of water. J Mater Chem. 2000;12:1782–6.
6. Yuk J, Troczynski T. Sol–gel $BaTiO_3$ thin film for humidity sensors. Sens Actuat B. 2003;94:290–3.
7. Alcoutlabi M, McKenna GB. Effects of confinement on material behavior at the nanometer size scale. J Phys Condens Matter. 2005;17:R461–524.
8. Kohiki S, Takada S, Shimizu A, Yamada K, Higashijima H. Quantum-confinement effect of the optical and dielectric properties for mesocrystals of $BaTiO_3$ and $SrBiTa_2O_9$. J Appl Phys. 2000;88:6092–6.
9. Kinka M, Banys J, Bohlmann W, Bierwirth E, Hartmann M, Michel D, Volkel G, Poppl A. Dielectric spectroscopy of $BaTiO_3$

confined in MCM-41 mesoporous molecular sieve materials. J Phys IV France. 2005;128:81–5.
10. Wei X. Hydrothermal synthesis of $BaTiO_3$ thin films on nanoporous TiO_2 covered Ti substrates. J Cryst Growth. 2006;286:371–5.
11. Sidorchuk V, Khalameida S, Zazhigalov V, Gorelov B, Kotenok O, Makhno S. Mechanochemical synthesis and some properties of barium titanate nanoparticles. In: European Materials Research Society 2008 fall meeting, Warsaw, Symposium; 2008, p. 55.
12. Wada S, Narahara M, Hoshina T, Kakemoto H, Tsurumi T. Preparation of nm-sized $BaTiO_3$ particles using a new 2-step thermal decomposition of barium titanyl oxalate. J Mater Sci. 2003;38:2655–60.
13. Khalameida S, Sydorchuk V, Skubiszewska-Zięba J, Leboda R, Zazhigalov V. Synthesis, thermoanalytical and spectroscopical studies of dispersed barium titanate. J Therm Anal Calorim. 2010. doi: 10.1007/s10973-010-0755-3.
14. Otta S, Bhattamisra SD. Kinetics and mechanism of the thermal decomposition of barium titanyl oxalate. J Therm Anal Calorim. 1994;41:419–33.